Graphene-diamond interface: Gap opening and electronic spin injection

Yandong Ma, Ying Dai, Meng Guo, and Baibiao Huang

Phys. Rev. B **85**, 235448 — Published 25 June 2012

DOI: 10.1103/PhysRevB.85.235448

Graphene-Diamond Interface: Gap Opening and Electronic Spin Injection

Yandong Ma, Ying Dai* , Meng Guo, and Baibiao Huang

School of Physics, State Key Laboratory of Crystal Materials, Shandong University,

Jinan 250100, People's Republic of China

Abstract

Creating a finite band gap, injecting electronic spin and finding a suitable substrate are the three important challenges for building graphene-based devices. Here, first-principles calculations are performed to investigate the electronic and magnetic properties of graphene adsorbed on the (111) surface of diamond, which is synthesized experimentally [Nature **472**, 74 (2011); J. Appl. Phys. **110**, 044324 (2011); Nano Lett. **12**, 1603 (2012); ACS Nano **6**, 1018 (2012)]. Our results unveil that the graphene adsorbed on diamond surface is a semiconductor with a finite gap depending on the adsorption arrangements due to the variation of on-site energy induced by diamond surface, with extra advantage of maintaining main characters of the linear band dispersion of graphene. More interestingly, different from typical graphene/semiconductor hybrid systems, we find that electronic spin can arise "intrinsically" in graphene owe to the exchange proximity interaction between electrons in graphene and localized electrons in diamond surface, rather than the characteristic graphene states. These predications strongly revive this new synthesized system as a viable candidate to overcome all the aforementioned challenges, providing an ideal platform for future graphene-based electronics.

* E-mail: daiy60@sina.com

Keywords: density functional theory; graphene; diamond; interface; gap opening.

I. Introduction

Owning to its high carrier mobility and saturation velocity, graphene has attracted enormous attention in recent years.[1-4] In particular, high-performance graphene transistors for radio-frequency applications are of great interest.[5–7] However, the lack of a finite band gap implies that the current can never be turned off completely and therefore devices fabricated from it have a small on-off ratio, whereas a potential graphene-based field effect transistor (FET) is expected to show only modest on-off ratio.[8] This has constituted a formidable obstacle on the way to the use of graphene in logic and high-speed switching devices.[9,10] Hence, huge efforts have been devoted to the creation of a tunable gap in graphene systems. Different approaches have been proposed, such as the cutting of 2D graphene into finite sized 1D nanoribbons,[11,12] control of the patterned hydrogenation,[13,14] application of uniaxial strain,[15,16] growth of epitaxial graphene on substrates,[17,18] and use of molecule doping.[19] However, compared with these intensive research efforts, the development of a reliable technique to create a finite gap without degrading the main characters of the linear band dispersion of the graphene remains challenging.

Electronic spin injection in graphene to induce magnetism "intrinsically" in graphene is another subject of intense interest at present.[20] However, the conventional approaches of magnetic modulation to induce magnetism, such as introducing transition metal atoms, point defects, and nonmetal element adsorption,[21-23] cannot

readily be applied to produce high-speed graphene transistors for many applications because they often introduce significant defects into the monolayer of carbon lattices and severely degrade the device performance.[7] Thus, other new efficient spin injection strategy into graphene is required for the realization of a prototypical spintronic device. The dream now becomes possible after the discovery of exploitation of the interfacial proximity with a ferromagnetic semiconductor. Indeed, it has been proposed that a spin splitting can arise in graphene just due to exchange proximity interaction between electrons in graphene and localized electrons in a semiconductor adjacent to graphene, rather than the characteristic graphene states.[24,25] The interaction approach could hereby serves as a flexible method to produce high performance graphene-based spintronics not previously possible in future spintronic applications. In view of this, the quest for such spin injection systems is very desirable and challenge for the development of spintronics.

Devices made from graphene should be supported on an ideal substrate, which is another important challenge for development of graphene-based electronics.[26] Graphene is very vulnerable to external condition, and its remarkable high electronic mobility can be affected by nearby materials. Previous studies on graphene-based devices typically use SiO_2 and SiC as the substrates.[6,7] However, graphene devices fabricated on them have been found to suffer from additional scattering associated with low surface phonon energy and large trap density,[27] resulting in deterioration of both devices properties and uniformity across the wafer. To mitigate these problems, it is critical to look for the best substrate on which to mount graphene for more practical

applications.

Very recently, the graphene/diamond hybrid system [GDH] has attracted extensive experimental attention and was successfully synthesized experimentally.[28-31] The replacing SiO_2 substrate with diamond helps one to substantially improve the radio frequency characteristics of the graphene transistors, leading to the new planar sp^2-on-sp^3 carbon-on-carbon technology. Compared to SiO_2 and most other substrates, diamond has characters of high phonon energy and low surface trap density.[28,29] Such desirable properties have ensured diamond as a suitable substrate material for graphene and provide a potential solution to overcome the aforementioned challenges. However, compared with the progress in experimental fabrications of GDH, its underlying characteristics of the interaction from a theoretical point of view are still far from being explained.

Stimulated by these challenges, it is necessary to examine the electronic and magnetic properties of the new synthesized GDH. In the present work, on the basis of density functional calculations, we systematically investigate whether a finite gap can be induced and whether electronic spin can be "intrinsically" injected in graphene if it contacts with diamond surface. Furthermore, the possible underlying physical mechanisms are discussed in detail.

II. Computational Methods

Note that in the absence of strong bonding interactions between the graphene and substrate, nonbonding van der Waals (vdW) forces are expected to be important. Thus, one needs to be cautious in dealing with problems of graphene adsorption on

semiconductor surface since the energetics might be affected by the vdW interactions that are missing in traditional density functional calculations. In the present studies, all our calculations, including geometry relaxation and electronic structure calculation, are based on a damped vdW correction (DFT-D2) proposed by Grimme[32] as implemented self consistently in Vienna *ab initio* Simulation Package (VASP).[33,34] For comparison, some calculations treat the exchange-correlation effect at the level of Perdew-Burke-Ernzerhof (PBE)[35] as implemented in the VASP. The plane-wave kinetic-energy cutoff is set at 500 eV. A vacuum layer of 18 Å is adopted in the direction normal to the interface, representing the isolated slab boundary condition. The Brillouin zone is represented by the set of 9×9×1 k-points[36] for both geometry optimizations and the static total energy calculations. Geometry optimization has been performed for all systems until the residual forces are converged to 0.02 eV/Å.

The cohesive energy per C atom between graphene and diamond surface is calculated as $E_{coh} = (E_{GDH} - E_G - E_D)/8$,where E_{GDH} , E_G , and E_D represent the total energy of the hybrid system, the pure graphene, and the pure diamond (111) surface, respectively.

III. Results and Discussion

To simulate a hybrid structure of GDH, we chose the (111) surface of diamond possessing a triangular lattices of C atoms at the most top layer. The surface is modeled by a slab contains six C bilayers with H passivation on the second surface of the slab. We imposed a commensurability condition between the graphene and diamond (111) surface, where a 2×2 lateral periodicity of the graphene and 2×2 lateral

periodicity of the diamond surface are employed. To bring focus to the fundamental properties of graphene adsorbed on diamond, we choose a lateral lattice parameter for triangular lattice a = 4.940 Å that is optimized for isolated graphene. The approximation made by this procedure is reasonable, since the mismatch with the optimized diamond surface parameters is only about 2%. And in order to investigate how the energetic and electronic structures of graphene depend on the local configuration on diamond surface, three stacking patterns are considered: (1) four C atoms of graphene are placed on the hollow sites of the surface bilayer [*H* configuration, as shown in **Figure 1a** and **1d**]; (2) four C atoms of graphene are placed directly above the C atoms of the second layer [*T* configuration, as shown in **Figure 1b** and **1e**]; (3) four C atoms of graphene are placed on the bridge sites of the surface bilayer [*B* configuration, as shown in **Figure 1c** and **1f**].

Figure 1 illustrates the fully optimized geometric structures of graphene adsorbed on the diamond surfaces. In all cases, graphene keeps its plane and hexagonal atomic network, maintaining the interlayer spacing of 2.957 Å, 2.807 Å, and 2.781 Å for *H*, *T*, and *B* configurations, respectively, when bonded to the diamond surface. The optimal interlayer spacing is found to be larger than the typical length of the C-C bonds, indicating that the bonds between graphene and diamond are absent in all the hybrid structures. Compared with the atomic structures of pure diamond (111) surface, the atomic structures of the diamond (111) surface with or without graphene layer are almost the same, indicating the weak interaction between them. On the other hand, it is found that the fluctuation of C atoms in graphene along the direction normal to

graphene plane is less than 0.02 Å, in contrast to the case of often used substrate SiC, in which a significant deformation of graphene plane usually happens.[17] As listed in **Table 1**, at the optimized interlayer spacing, the calculated cohesive energy per C atom in *H*, *T*, and *B* configurations are -17.6 meV, -14.5 meV, and -13.3 meV, respectively. These results indicate that the energetic of graphene on the diamond surface are slightly sensitive to the adsorption site. The adsorption arrangement dependency of the energetics of GDH is different from the adsorption of grphene on MoS_2 and $MoSe_2$ monolayers,[18,37] in which the cohesive energy is equal irrespective of the adsorption configurations. This discrepancy probably arises from the difference between the surface with and without dangling bonds. Based on the analysis above, it thus can be concluded that the graphene is loosely bonded to the diamond surface.

To show the effect of vdW interaction in such systems, the cohesive energy and relaxed geometric parameters without vdW interactions are also listed in **Table 1**. It is shown that, the resulting values of interlayer spacing are 3.338 Å, 3.201 Å, and 3.218 Å for *H*, *T*, and *B* configurations using the PBE, respectively. While the corresponding values of cohesive energy per C atom are -1.2 meV, -1.5 meV, and -3.4 meV, respectively. There is a significantly difference between the results with inclusion and without inclusion of vdW interactions, which indicates incorporation of the vdW interaction is extremely important for accurately describing the geometric structures of the GDH.

Now question arises, since the interaction between graphene and diamond surface is weakly, whether the electronic structures of graphene can be affected by diamond

surface in GDH. To answer this question, it thus is necessary to study the electronic properties of GDH. However, in order to have a concept about the electronic structures of the subdivisions of GDH, it is instructive to first examine the electronic properties of pure graphene and diamond clean surface. As **Figure 2a** illustrates, graphene is a gapless semiconductor, the (bonding) π bands and (antibonding) π^* bands cross only at the corners of the hexagonal Brillouin zone of the system, so-called *K* points. While for diamond (111) surface, since the surface carbon atoms are unhydrogenated, the localized states in the supercell would generate a total magnetic moment of 4.0 μ_B, arising from the contracted nature of the C 2*p* states. The total magnetic moment is mainly contributed by the surface unhydrogenated carbon atoms (0.538 μ_B/atom), and the carbon atoms of the third layer (0.200 μ_B/atom) due to the structural relaxation. Besides, other atoms in the supercell also have some contribution to the total magnetic moment. To study the preferred coupling of these moments, we consider the following three configurations: (1) ferromagnetic (FM) coupling; (2) antiferromagnetic (AFM) coupling; and (3) nonmagnetic (NM) state, where the calculation is spin unpolarized. We find that the ground state to be FM, and the corresponding electronic structure is presented in **Figure 2b** and **2c**. It can be seen the spin up channel is located at low energy relative to the spin down channel, but the two share similar distribution in reciprocal space.

For the graphene/diamond hybrid system, the calculated electronic band structures with *H*, *T*, and *B* configurations are plotted in **Figure 3**. We find that, most noticeably, spin polarization can be induced in the epitaxial graphene by the diamond surface.

Besides, the corresponding electronic band structures of isolated graphene taken from *H*, *T*, and *B* configurations display symmetric characteristic for the majority and minority projections of the spin. The total magnetic moments of isolated graphene are zero, indicating the local magnetic moment cannot form in a isolated graphene. At this point, clearly, the isolated graphene taken from *H*, *T*, and *B* configurations are nonmagnetic. Thus any spin polarization induced in graphene must originate from the interfacial proximity with diamond surface. Such interesting phenomena is different from the typical graphene/semiconductor hybrid systems in which no spin polarization could be induced in the epitaxial graphene by the substrate. Injection of spin in graphene is the current subject of intense investigation efforts. Although spin injection in graphene could also be induced by an external electric field or transition metal doping,[21,38] the required electronic field is so strong and heavy transition-metal elements also often act as poison agents in biological systems. On the other hand, the manipulation of the substrate can be not only used to tune the spins but also to control the charge carries of graphene. As **Figure 3** illustrates, most of the characters of the electronic energy band of pristine monolyaer graphene can still be seen clearly. However, focuing on the bands near the Fermi level at the *K* points, it reveals that the π and π^* bands repulse each other, forming a finite energy gap at the *K* points. Thus, the graphene adsorbed on the diamond surface is no longer metallic with massless electrons, but semiconducting with a direct narrow fundamental gap. From the insert in **Figure 3**, it can be seen that the gap in the spin-up (spin-down) state of the epitaxial graphene is calculated to be 388 meV (459 meV), 581 meV (767 meV), and

460 meV (508 meV), respectively, for the *H*, *T*, and *B* configurations. It should be noted that, due to the small differences in binding energies between the three different stackings, in combination with the lattice mismatch of around 2%, graphene may not adjust itself to some stacking configuration when placed on diamond, but every stacking sequence would be presented. Since the absence of a finite band gap without degrading the electronic properties of the graphene is a significant obstacle in construction of graphene-based FET, our results make the GDH promising as an electronic material. Furthermore, these gap values are significantly larger than k_BT at room temperature, indicating the achievable of current on/off ratio is larger than that of the freestanding graphene. Our results here strongly suggest that the GDH system could have strong potential to overcome the aforementioned challenges. It is important to note here that such GDH has been already fabricated experimentally,[28-31] indicating that actual applications of such hypothetical devices may be realizable in the near future.

Now one may ask: "what makes the semiconducting properties of graphene on diamond surface?" These features are understandable in terms of the π-electron tight-binding approximation of graphene. According to this model, the variation in onsite energy of C atom in graphene induced by the diamond surface disrupts the degeneracy of the π and π^* bands at the *K* point, resulting in their semiconducting character. In order to unravel more information about the bonding mechanism, it is worthwhile to investigate charge density difference, $\Delta\rho = \rho(GDH) - \rho(G) - \rho(D)$, constructed by subtracting the calculated electronic charge of the GDH from that of

the independent diamond surface and graphene. Here, the structure of the independent diamond surface and graphene is taken to be the same as that of GDH. Plots of charge density difference for GDH in *H* configuration in **Figure 4** clearly show that charge density is redistributed by forming electron-rich and hole-rich regions within the graphene layer. And the formation of the electron-hole regions is understood as due to the inhomogeneous planar diamond surface which drives the interlayer charge transfer from diamond surface to graphene. Indeed, this result is also confirmed by the electronic band structure of graphene on diamond surface. As shown in **Figure 2a** and **Figure 3a** and **3b**, when compared to the band structure for the isolate graphene, clearly, we notice that the graphene on diamond surface is slightly n-doped, attributing to the electron transfer from the diamond surface to graphene. Besides, as shown in **Figure 4a** in which green (yellow) isosurfaces represents charge depletion (accumulation), a slight but significant accumulation in the spacious region between graphene and diamond surface is also observed, resulting from the interaction between graphene and diamond surface.

At last we turn our attention to get a physical insight into the interesting electronic spin injection in graphene inducing magnetism "intrinsically" in graphene. As mentioned above, the isolated graphene taken from *H*, *T*, and *B* configurations are nonmagnetic. Thus any spin polarization induced in graphene must originate from the interfacial proximity with diamond surface. Furthermore, from the aforementioned analysis, it is shown that the charge transfer between graphene and diamond surface is significant. Given the consideration of these factors, it can be proposed that this

interesting phenomenon arises from the effect of the through-space exchange interaction. For the through-space exchange interaction, it is defined that a material with specific properties induces similar characters on the adjacent material through charge transfer between the two materials. Provided that α and β represent the materials with and without specific properties, according to the through-space exchange interaction, an electron without such properties from β transfers along the β-α-$(\beta$-$\alpha)_n$-β(n=1, 2, 3…) path. When the electron returns back to β, the characters of α would be simultaneity transferred to β. Consequently, the through-space exchange interaction would induce the similar characters in β. As expected from this mechanism, for the GDH system, the basic principle underlying the interesting spin injection in graphene can be understood by considering processes in which an electron from graphene tunnels onto diamond surface, whereupon it obtains enormous spin polarization density, and then returns to the graphene. Such process effectively enhances the graphene's spin polarization strength. Besides, the revealed mechanism of the spin injection provides the necessary insight for the future studies of graphene-based electronic devices.

IV. Summary

In summary, we have investigated the electronic and magnetic properties of graphene adsorbed on diamond (111) surface based on density functional theory. Although graphene is loosely bonded to the diamond surface with the interlayer spacing of 2.957 Å, 2.807 Å, and 2.781 Å for *H*, *T*, and *B* configurations, respectively, the electronic structures of graphene can be significantly affected by diamond surface

in GDH:

(1) The graphene adsorbed on diamond surface is a semiconductor with a finite gap due to the variation of on-site energy induced by diamond surface, with extra advantage of maintaining main characters of the linear band dispersion of graphene. And the gap values depend on the stacking pattern, which is different from that for graphene adsorbed on MoS_2 and $MoSe_2$. Furthermore, these gap values are significantly larger than k_BT at room temperature, indicating the achievable of current on/off ratio is larger than that of the freestanding graphene.

(2) Magnetism can arise "intrinsically" in graphene owe to the exchange proximity interaction between electrons in graphene and localized electrons in diamond surface, rather than the characteristic graphene states. Such interesting phenomena is different from the typical graphene/semiconductor hybrid systems in which no spin polarization could be induced in the epitaxial graphene by the substrate.

Our results are useful complement to experimental studies of this new synthesized system, revive this new synthesized system as a viable candidate to overcome all the aforementioned important challenges, and can lead to the new planar sp^2-on-sp^3 carbon-on-carbon technology.

Acknowledgement

This work is supported by the National Science foundation of China under Grant 11174180 and 20973102, and the Natural Science Foundation of Shandong Province under Grant number ZR2011AM009.

References and Notes

[1]K. S. Novoselov, et al. Nature **438**, 197 (2005).

[2]Y. B. Zhang, Y. W. Tan, H. L. Stormer, and P. Kim, Nature **438**, 201 (2005).

[3]C. Berger, et al. Science **312**, 1191 (2006).

[4]P. Avouris, Nano Lett. **10**, 4285 (2010).

[5]Y.-M. Lin, K. A. Jenkins, A. Valdes-Garcia, J. P. Small, D. B. Farmer, and P. Avouris, Nano Lett. **9**, 422 (2009).

[6]Y.-M. Lin, C. Dimitrakopoulos, K. A. Jenkins, D. B. Farmer, H.-Y. Chiu, A. Grill, and P. Avouris, Science **327**, 662 (2010).

[7]L. Liao, Y.-C. Lin, M. Q. Bao, R. Cheng, J. W. Bai, Y. Liu, Y. Q. Qu, K. L. Wang, Y. Huang, and X. F. Duan, Nature **467**, 305 (2010).

[8]K. S. Novoselov, D. Jiang, F. Schedin, T. J. Booth, W. Khotkevich, S. V. Morozov, and A. K. Geim, Proc. Nat. Acad. Sci., U.S.A. **102**, 10451 (2005).

[9]G. Brumfiel, Nature **458**, 390 (2009).

[10]T. P. Kaloni, Y. C. Cheng, and U. Schwingenschlögl, J. Mater. Chem. **22**, 919 (2012).

[11]D. V. Kosynkin, A. L. Higginbotham, A. Sinitskii, J. R. Lomeda, A. Dimiev, B. K. Price, and J. M. Tour, Nature **458**, 872 (2009).

[12]L. Jiao, L. Zhang, X. Wang, G. Diankov, and H. Dai, Nature **458**, 877 (2009).

[13]R. Balog, B. Jørgensen, L. Nilsson, M. Andersen, E. Rienks, M. Bianchi, M. Fanetti, E. Lægsgaard, A. Baraldi, S. Lizzit, Z. Sljivancanin, F. Besenbacher, B. Hammer, T. G. Pedersen, P. Hofmann, and L. Homekaer, Nat. Mater. **9**, 315 (2010).

[14]Y. D. Ma, Y. Dai, M. Guo, C. W. Niu, Z. K. Zhang, and B. B. Huang, Phys. Chem.

Chem. Phys. **14**, 3651 (2012).

[15]F. Guinea, M. I. Katsnelson, and A. Gerim, Nat. Phys. **6**, 30 (2010).

[16]Z. H. Ni, T. Yu, Y. H. Lu, Y. Y. Wang, Y. P. Feng, and Z. X. Shen, ACS Nano **2**, 2301 (2008).

[17]A. J. Du, et al. J. Am. Chem. Soc. **134**, 4393 (2012).

[18]Y. D. Ma, Y. Dai, M. Guo, C. W. Niu, and B. B. Huang, Nanoscale **3**, 3883 (2011).

[19]W. J. Zhang, C. T. Lin, K. K. Liu, T. Tite, C. Y. Su, C. H. Chang, Y. H. Lee, C. W. Chu, K. H. Wei, J. L. Kuo, and L. J. Li, ACS Nano **9**, 7517 (2011).

[20]N. Tombros, C. Jozsa1, M. Popinciuc, H. T. Jonkman, and B. J. V. Wees, Nature **448**, 571 (2007).

[21]A. V. Krasheninnikov, P. O. Lehtinen, A. S. Foster, P. Pyykko, and R. M. Nieminen, Phys. Rev. Lett. **102**, 126807 (2009).

[22]Y. D. Ma, Y. Dai, M. Guo, C. W. Niu, Y. T. Zhu, and B. B. Huang, ACS Nano **6**, 1695 (2012).

[23]J. S. Crvenka, M. I. Katsnelson, and C. F. J. Flipse, Nat. Phys. **5**, 840 (2009).

[24]Y. Semenov, K. Kim, and J. Zavada, Appl. Phys. Lett. **91**, 153105 (2007).

[25]H. Huegen, D. Huertas-Hernando, and A. Brataas, Phys. Rev. B **77**, 115406 (2008).

[26]R. Decker, Y. Wang, V. W. Brar, W. Regan, H. Z. Tsai, Q. Wu, W. Gannett, A. Zettl, and M. F. Crommie, Nano Lett. **11**, 2291 (2011).

[27]L. A. Ponomarenko, R. Yang, T. M. Mohiuddin, M. I. Katsnelson, K. S. Novoselov, S. V. Morozov, A. A. Zhukov, F. Schedin, E. W. Hill, and A. K. Geim, Phys. Rev. Lett. **102**, 206603 (2009).

[28]Y. Q. Wu, Y. M. Lin, A. A. Bol1, K. A. Jenkins, F. N. Xia, D. B. Farmer, Y. Zhu, and P. Avouris, Nature **472**, 74 (2011).

[29]J. Yu, G. X. Liu, A. V. Sumant, V. Goyal, and A. A. Balandin, Nano Lett. **12**, 1603 (2012).

[30]Y. Wang, M. Jaiswal, M. Lin, S. Saha, B. Özyilmaz, and P. K. Loh, ACS Nano **6**, 1018 (2012).

[31]D. Varshney, C. V. Rao, M. J.-F. Guinel, Y. Ishikawa, B. R. Weiner, and G. Morell, J. Appl. Phys. **110**, 044324 (2011).

[32]S. Grimme, J. Comput. Chem. **27**, 1787 (2006).

[33]G. Kresse and J. Furthmuller, Phys. Rev. B **54**, 11169 (1996).

[34]G. Kresse and J. Joubert, Phys. Rev. B **59**, 1758 (1999).

[35]J. P. Perdew, K. Burke, and M. Ernzerhof, Phys. Rev. Lett. **77**, 3865 (1996).

[36]H. J. Monkhorst and J. D. Pack, Phys. Rev. B **13**, 5188 (1976).

[37]Y. D. Ma, Y. Dai, M. Guo, C. W. Niu, L. Yu, and B. B. Huang, J. Phys. Chem. C **115**, 20237 (2011).

[38]P. Michetti, P. Recher, and G. Iannaccone, Nano Lett. **10**, 4463 (2010).

Table 1. Optimized interlayer distance d (Å) and the cohesive energy per C atom E_{coh} (meV) of graphene on the diamond surface in different configurations.

	DFT-D2		PBE	
Configuration	d	E_{coh}	d	E_{coh}
H	2.975	-17.6	3.338	-1.2
T	2.807	-14.5	3.201	-1.5
B	2.781	-13.3	3.218	-3.4

Figure captions:

Figure 1. Equilibrium structure of graphene supported on diamond surface from top and side views for *H* (a, d), *T* (b, e), and *B* (c, f) configurations. Only the topmost bilayer of diamond surface is shown. The graphene, topmost layer of diamond surface and second layer of diamond surface are hilighted in blue, red and orange, respectively.

Figure 2. The electronic band structures of (a) graphene and [(b) and (c)] diamond (111) surface. The (b) and (c) represent the spin-up and spin-down states, respectively. The Fermi level is set at zero energy.

Figure 3. Electronic band structures of [(a) and (b)] GDH in *T* configuration, [(c) and (d)] GDH in *B* configuration, and [(e) and (f)] GDH in *H* configuration. The orange line and dark cyan line represent the spin-up and spin-down states, respectively. The horizontal dashed lines indicate the Fermi level. Insert: the gap of graphene near the *K* point induced by diamond surface. The linear energy dispersion of the graphene in the corresponding GDH around the Fermi energy (blue dotted line) is also plotted for reference.

Figure 4. (a) Side and (b) top views of the three-dimensional charge density difference plots. Green and yellow isosurfaces represent charge depletion and accumulation in the space with respect to isolated graphene and diamond surface, respectively.

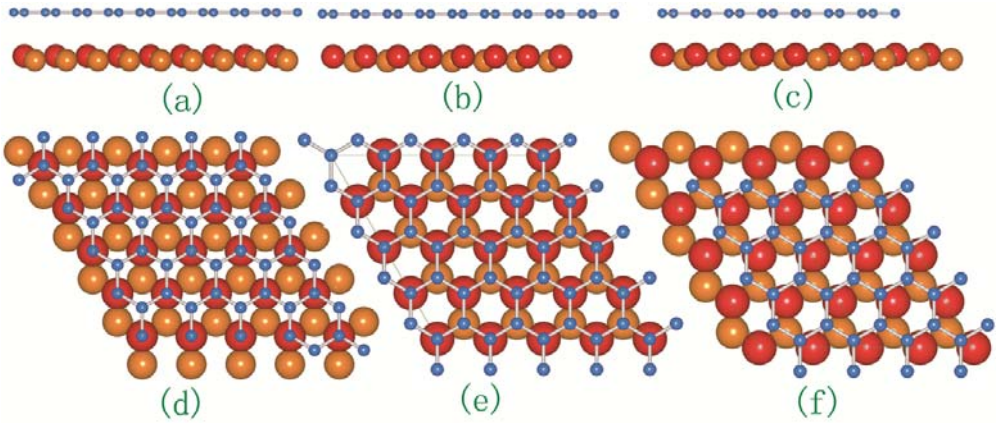

Figure 1. Equilibrium structure of graphene supported on diamond surface from top and side views for *H* (a, d), *T* (b, e), and *B* (c, f) configurations. Only the topmost bilayer of diamond surface is shown. The graphene, topmost layer of diamond surface and second layer of diamond surface are hilighted in blue, red and orange, respectively.

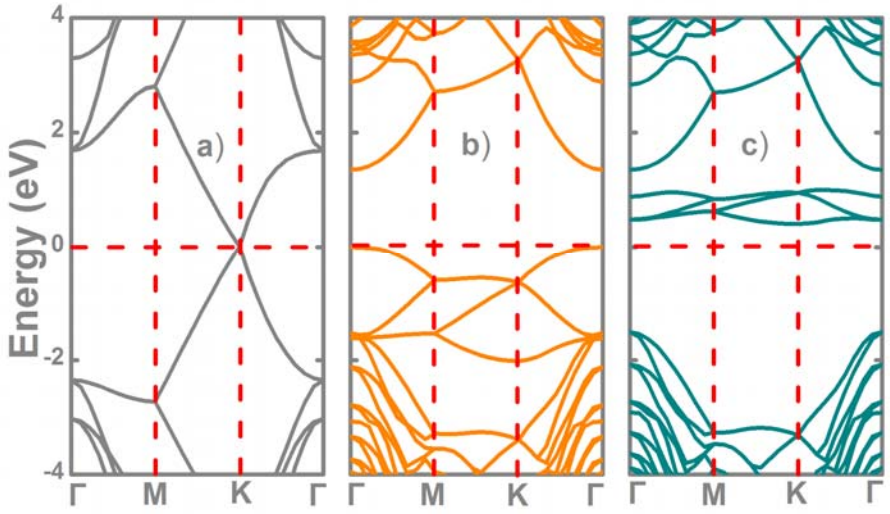

Figure 2. The electronic band structures of (a) graphene and [(b) and (c)] diamond (111) surface. The (b) and (c) represent the spin-up and spin-down states, respectively. The Fermi level is set at zero energy.

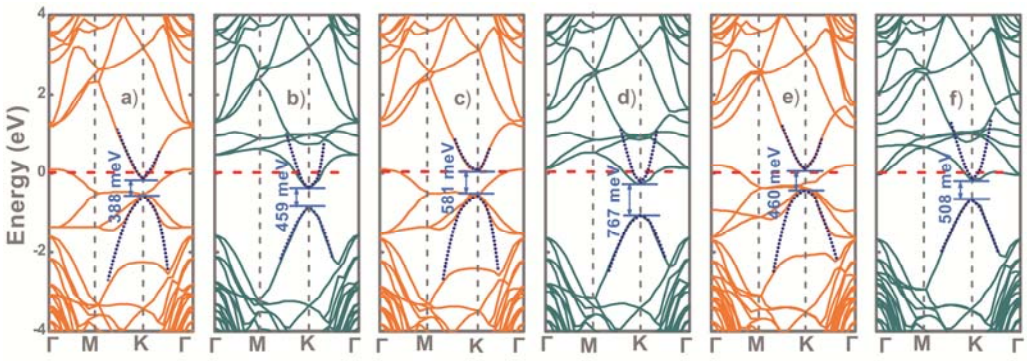

Figure 3. Electronic band structures of [(a) and (b)] GDH in *T* configuration, [(c) and (d)] GDH in *B* configuration, and [(e) and (f)] GDH in *H* configuration. The orange line and dark cyan line represent the spin-up and spin-down states, respectively. The horizontal dashed lines indicate the Fermi level. Insert: the gap of graphene near the *K* point induced by diamond surface. The linear energy dispersion of the graphene in the corresponding GDH around the Fermi energy (blue dotted line) is also plotted for reference.

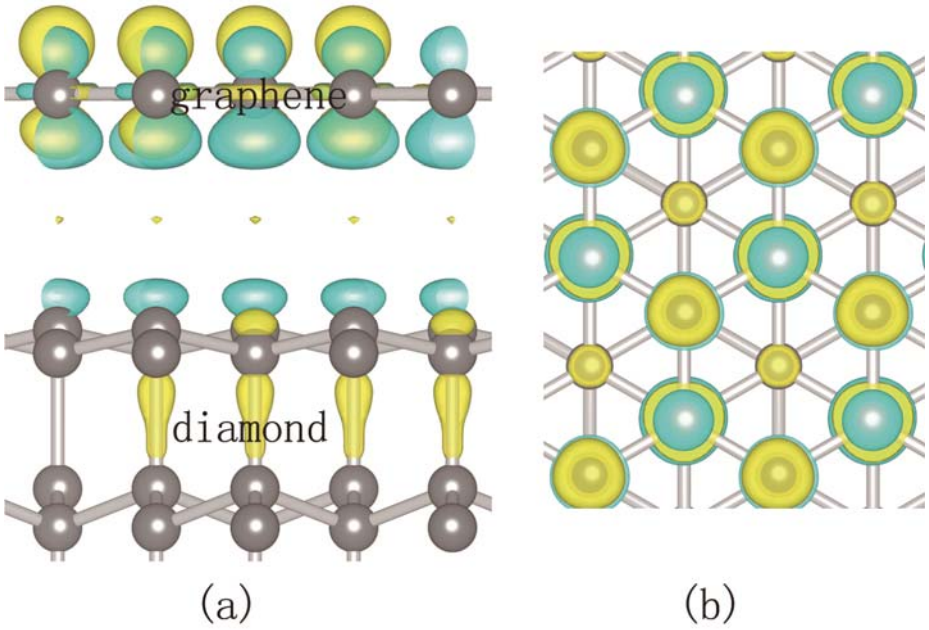

Figure 4. (a) Side and (b) top views of the three-dimensional charge density difference plots. Green and yellow isosurfaces represent charge depletion and accumulation in the space with respect to isolated graphene and diamond surface, respectively.